Synthesis and Characterization of New Liquid-Crystalline Block Copolymers with *p*-Cyanoazobenzene Moieties and Poly(*n*-butyl acrylate) Segments Using Atom-Transfer Radical Polymerization

Yang-Kyoo Han,*,†,‡ Bruno Dufour,† Wei Wu,† Tomasz Kowalewski,† and Krzysztof Matyjaszewski*,†

Center for Macromolecular Engineering, Department of Chemistry, Carnegie Mellon University, 4400 Fifth Avenue, Pittsburgh, Pennsylvania 15213 and Center for Functionalized Organics and Organic-Inorganics, Department of Chemistry, Hanyang University, Sung-dong Gu, Seoul 133-791, Korea

Received April 23, 2004; Revised Manuscript Received September 7, 2004

ABSTRACT: Homopolymers with side-chain liquid-crystalline units (LC) were prepared by ATRP of a LC monomer, 2-[2-(4-cyano-azobenzene-4′-oxy)ethylene-oxy]ethyl methacrylate. The resulting polymers had low polydispersity, $M_w/M_n < 1.2$. Optical and thermal investigation confirmed that both the monomer and the homopolymers have smectic structures. New di- and triblock copolymers containing LC units, with different ratios of the block containing the LC monomer with azobenzene moiety, and poly(*n*-butyl acrylate) as a soft segment were successfully prepared using ATRP. The block copolymerization proceeded with controlled/living characteristics. The morphologies of thin films of the block copolymers cast from different solvents were examined by atomic force microscopy using different casting procedures. Whereas the observed morphologies were similar to those observed in conventional block copolymers, particularly strong dependence on sample preparation conditions and thermal history was observed, suggesting the role of mesogenic blocks in stabilization of metastable states.

Introduction

Atom-transfer radical polymerization (ATRP), one of the systems developed for controlled/living radical polymerization (CRP),[1,2] has been the subject of a number of studies.[3−5] One of the reasons is that ATRP provides several advantages over conventional living anionic polymerization, in particular the ease with which it can be applied to a wide variety of monomers ranging from styrene to water-soluble acrylamide.[6−13] The method also provides polymers with low polydispersities, even at relatively high reaction temperatures.[14,15] In addition, unlike living anionic polymerization,[16−18] ATRP facilitates preparation of well-defined diblock and triblock copolymers from (meth)acrylate monomers with various reactivity ratios.

Block copolymers containing rigid and soft blocks may behave as thermoplastic elastomers (TPE). TPEs usually have an ABA structure with domains composed of rigid (e.g., crystalline) A blocks, dispersed in a soft matrix formed by B blocks. Incorporation of flanking A segments from any given chain into different phase-separated A domains facilitates physical cross-linking of the system, resulting in materials with elastomeric properties. Unlike chemically cross-linked rubbers, which cannot be processed without breaking covalent bonds, the TPEs can be processed in the melt above their order−disorder temperature (ODT) and also dissolved in appropriate solvents. Due to these advantages, a number of TPE block copolymers have been prepared by ATRP and studied extensively.[19−25] Polymers used typically as soft blocks include polyisoprene, polybutadiene, poly(dimethylsiloxane), poly(tetramethylene glycol), and poly(*n*-butyl acrylate). Polymers employed as hard blocks may include not only obvious choices such as polystyrene, polyacrylonitrile, polyurethane, and polyethylene, but also poly(meth)acrylates with long alkyl chains such as octadecyl (stearyl) groups, and plausibly also liquid-crystalline (LC) polymers. Prior to the development of ATRP, research on block copolymers consisting of incompatible LC segments and amorphous blocks has been very limited due to the difficulties in synthesis of such materials via living anionic polymerization.[26] With the availability of ATRP, the synthesis of block copolymers composed of azobenzene-containing LC block and soft segment has recently received more attention.[27−32] Of particular interest with these materials is the potential ability to control their microphase-separated morphologies (spheres, cylinders, lamellae) and their domain sizes by the photoisomerization of azobenzene groups in the block copolymers and by different thermal treatment of the LC block.[33,34] Azobenzene-containing polymers have been widely applied in the fields of optical switching, optical data storage, and photonic memories through the photoinduced trans−cis isomerization of the light-sensitive azobenzene chromophore.[35−37] Incorporation of these segments into block copolymers is expected to provide the additional possibilities to control the properties of optoelectronic materials.

In this paper we report the ATRP synthesis of LC homopolymers with azobenzene moiety and their block copolymers with *n*-butyl acrylate and the characterization of thermal properties and morphology of these materials. In addition, we describe the influence of temperature and solvent on the morphologies of block copolymers with different ratios of LC monomer to comonomer in the A-block(s).

Experimental Section

Materials. 4-Aminobenzonitrile (Aldrich, 98%) was recrystallized from a mixture of water and ethanol (9/1, v/v). Copper-

* To whom correspondence should be addressed.
† Carnegie Mellon University.
‡ Hanyang University.

10.1021/ma0492059 CCC: $27.50
Published on Web 11/06/2004

Scheme 1. Synthetic Route to LC Monomer and Homopolymer

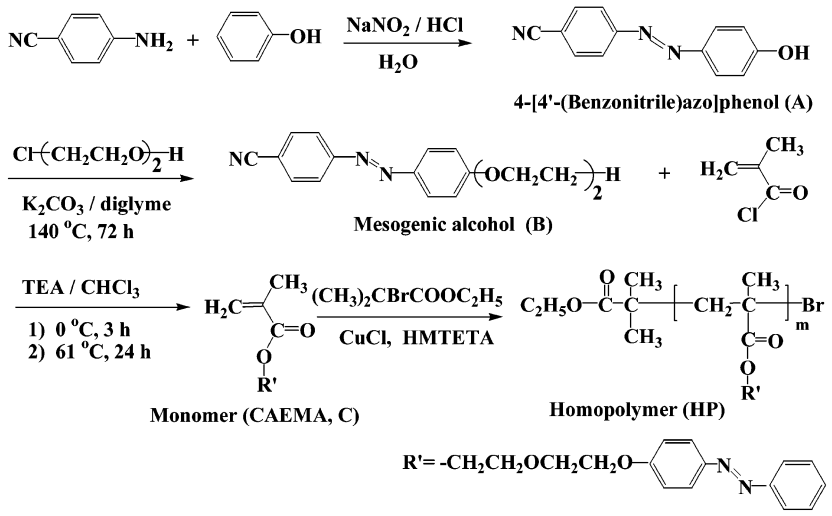

(I) chloride and copper(I) bromide were purified as reported in our previous report.[38] *N*,*N*,*N*′,*N*″,*N*″-Pentamethyldiethylenetriamine (PMDETA, 99%), 1,1,4,7,10,10-hexamethyltriethylenetetraamine (HMTETA, 97%),[39] ethyl 2-bromoisobutyrate (EBriB, 98%), methyl 2-bromopropionate (MBrP, 98%), dimethyl 2,6-dibromoheptanedioate (DMDBHD, 97%), sodium nitrite (97+%), and 2-(2-chloroethoxy)ethanol (99%) were used as received (Aldrich). *n*-Butyl acrylate (BA) (Aldrich, 99%) was passed through a column filled with neutral alumina to remove stabilizer, dried over calcium hydride, and then distilled under reduced pressure before use. Anisole was distilled over calcium hydride under nitrogen prior to use. All other reagents and solvents were used as received.

Characterization. Molecular weights and molecular weight distributions were measured by gel permeation chromatography (GPC) with a series of three polystyrene standard columns (Styragel, 10^5, 10^3, 10^2 Å) and a Waters 2410 differential refractometer using THF as an eluent (flow rate of 1 mL/min, 30 °C). Linear polystyrene standards were used for calibration of molecular weights of all polymers. ^{1}H NMR spectra in $CDCl_3$ were recorded on a Bruker spectrometer (300 MHz) using TMS as a reference solvent. Conversion of monomer to polymer in the synthesis of macroinitiator of poly(*n*-butyl acrylate) was determined on a Shimadzu GC-14A gas chromatograph equipped with a flame ionization detector and a capillary column (J&W Scientific 30 m DB WAX Megabore column). Thermal behavior of monomer and polymer was measured by a differential scanning calorimeter (TA Instruments DSC-Q 100) at a heating rate of 10 °C/min under nitrogen atmosphere. Birefringent textures of the prepared monomer and polymers were observed through an optical polarizing microscope (OPM, Leica, DMRXP-MPS 60) equipped with a hot stage. Atomic force microscopy (AFM) images were recorded with a Nanoscope III Multimode System (Digital Instruments) operating in tapping mode. The measurements were carried out at ambient conditions using standard silicon TESP probes with a spring constant of ca. 50 N/m and a resonance frequency of 300 kHz.

Synthesis of Monomer. The LC monomer with a side-chain azobenzene group, 2-[(4-cyano-azobenzene-4′-oxy)ethylene-oxy]ethyl methacrylate (CAEMA), was synthesized by a procedure modified from that described in the literature,[40,41] as shown in Scheme 1.

Synthesis of 4-[4′-(Benzonitrile)azo]phenol (A). Compound **A** was prepared by reaction of 4-aminobenzonitrile with phenol in the presence of sodium nitrite according to the published literature method.[42] Yield and melting point were 92% and 202 °C (lit. 203−205 °C), respectively.

Synthesis of Mesogenic Alcohol (B). The coupling reaction of 2-(2-chloroethoxy)ethanol with the synthesized compound **A** to prepare the mesogenic alcohol (**B**) was carried out according to the following procedure. A 3.0 g (0.014 mol) amount of compound **A**, 1.116 g (20% excess vs azophenol) of potassium carbonate, and 40 mL of diglyme solvent were placed into a two-necked round-bottom flask equipped with a water-cooled condenser and a drying tube and then stirred for 30 min at room temperature. A solution of 2-(2-chloroethoxy)-ethanol (2.513 g, 50% excess vs azophenol) in diglyme (20 mL) was slowly added to the mixture through a dropping funnel over a 20 min period. The solution was heated to 140 °C and then refluxed for 72 h. After the reaction was completed, the mixture was cooled to room temperature and then poured into a large amount of water (500 mL) to precipitate a solid. The filtered solid was added to acetone (300 mL), stirred for 3 h, and then filtered to remove any trace of compound **A** by dissolving it in acetone. The filtered crude product was recrystallized from ethanol over 3 days to obtain pure mesogenic alcohol.[40]

Yield: 75%. mp: 142−144 °C (lit. 141−143 °C). ^{1}H NMR ($CDCl_3$, 300 MHz): 7.9 (d, ArH, 4H), 7.7 (d, ArH, 2H), 7.0 (d, ArH, 2H), 4.3 (t, OCH_2−Ar, 2H), 3.9 (t, $COOCH_2$, 2H), 3.8 and 3.6 (t, CH_2OCH_2, 4H), and 2.1 (s, OH, H).

Synthesis of 2-[2-(4-Cyano-azobenzene-4′-oxy)ethylene-oxy]ethyl Methacrylate (CAEMA, C), a LC Monomer. A 2 g (6.4 mmol) amount of the mesogenic alcohol, 0.98 g (9.7 mmol, acid acceptor; 50% excess) of triethylamine, and 40 mL of chloroform were placed in a two-necked round-bottom flask equipped with a water-cooled condenser with a drying tube and then stirred for 1 h at 40 °C to dissolve them completely. The clear solution was cooled to 0 °C, and a solution of methacryloyl chloride (1.254 g, 0.129 mol, 200% vs the mesogenic alcohol) in chloroform (20 mL) was slowly added to the solution through a dropping funnel over 20 min at 0 °C and then stirred for 3 h, keeping the reaction temperature between 0 and 5 °C. The solution was heated to 61 °C and refluxed for 24 h. After the reaction was completed, the solution was cooled to room temperature. The solution and 5% sodium bicarbonate water solution (100 mL) were added to a 500 mL separating funnel and then shaken vigorously to remove any excess of methacryloyl chloride and triethylamine salt generated during the reaction. The chloroform organic layer was washed with distilled water (100 mL) three times or until the solution became neutral. The organic layer was dried over anhydrous magnesium sulfate to remove any water remaining in the solution. After removing the solvent from the filtrate, the yellowish crude solid was purified by passing through a silica gel column using a mixed solvent of ethyl acetate and chloroform (1/5, v/v) as the developing solvent. The first 200 mL of elution volume during the column chromatography was collected, and then the solvents were removed by distillation to yield a yellowish monomer.

Yield: 59%. mp: 73−75 °C. ^{1}H NMR ($CDCl_3$, 300 MHz): 7.9 (d, ArH, 4H), 7.7 (d, ArH, 2H), 7.0 (d, ArH, 2H), 6.1 and 5.5 (s, $=CH_2$, 2H), 4.3 (t, OCH_2−Ar, 2H), 4.2 (t, $COOCH_2$, 2H), 3.9 and 3.8 (t, CH_2OCH_2, 4H), and 1.9 (s, CCH_3, 3H).

Table 1. Homopolymerization of LC CAEMA and Block Copolymerization with BA by ATRP

sample[a]	$[M]_o/[I]_o/[C]_o/[L]_o$[b]	solvent (mol/L)[c]	time (h)	conv. (%)[d]	M_n (GPC)[e]	M_n (calcd)[f]	M_w/M_n (GPC)[e]	LC content (%)[g]
HP-1	60/1/2/2	0.2	25	34.8	8 100	8 154	1.09	100
HP-2[h]	60/1/2/2	0.2	25	54.4	11 900	12 565	1.10	100
HP-3	60/1/2/2	0.2	24	13.7	5 500	3 310	1.20	100
MMI[i]	1000/2/1/1	not used	23	**57.2**[j]	42 100		1.14	
DBC-1	60/1/2/2	0.15	18	16.1	43 500	45 761	1.15	4.2
DBC-2	60/1/2/2	0.15	91	35.3	50 500	50 345	1.16	15.8
DMI[i]	400/1/1/1	not used	10	**50.1**[j]	24 700		1.13	
TBC-1	30/1/2/2	0.3	48	42.5	29 600	29 560	1.26	17.5
TBC-2	60/1/2/2	0.3	120	86.7	41 500	44 445	1.24	38.7
TBC-3	160/1/2/2	0.3	120	40.1	49 500	49 046	1.31	53.4

[a] HP, homopolymer; MMI, monofunctional macroinitiator (PBA-Br); DBC, diblock copolymer; DMI, difunctional macrinitiator (Br-PBA-Br); TBC, triblock copolymer. [b] Feed molar ratio; [M], monomer; [I], initiator; [C], catalyst; [L], ligand. [c] Monomer concentration vs solvent. [d] Determined by GPC. [e] On the basis of polystyrene standards. [f] Calculated from the equation $M_n(\text{calcd}) = \{[M]_o/[I]_o \times \text{conversion} \times 379\}$ + the molecular weight of initiator used, where 379 denotes the molecular weight of CAEMA monomer. [g] Determined by ^{1}H NMR. [h] Polymerization temperature = 90 °C; CuBr was used as catalyst instead of CuCl. [i] Bold entries describe the synthesis of monofunctional (PBA-Br) and difunctional (Br-PBA-Br) macroinitiators for the preparation of the block copolymers. [j] Determined by GC.

Preparation of Homopolymer (PCAEMA). A typical ATRP homopolymerization of the CAEMA was carried out as follows: 379 mg (1.0 mmol) of CAEMA and 5.0 mL of anisole solvent were placed into a 10 mL Schlenk flask fitted with rubber septa and purged with nitrogen for 20 min. A 3.7 μL (0.034 mmol) amount of HMTETA and 2.5 μL (0.017 mmol) of EBriB were added to the resulting solution through a microsyringe, and then the mixture was degassed with nitrogen for 10 min to remove air. Finally, 3.3 mg (0.034 mmol) of CuCl was placed into the reaction mixture, and it was degassed by three freeze−pump−thaw cycles. An initial sample (0.1 mL) was removed to confirm the elution volumes of monomer and solvent in the GPC curve before polymerization. The orange-colored reaction mixture was immersed in a silicone oil bath preheated to 80 °C. The turbid solution became clear and transparent within a few minutes. The clear solution was stirred at 80 °C under nitrogen atmosphere to conduct the polymerization. In specified time intervals the polymer solution in anisole was sampled by a syringe for GPC analysis. The polymerization was terminated by the addition of a large amount of THF (5 mL). The diluted solution was passed through an alumina column to remove the CuCl catalyst, and then the filtrate was precipitated by addition to a large volume of methanol (100 mL). The precipitated yellowish homopolymer (PCAEMA) was filtered and dried 60 °C for 24 h under vacuum. Conversion = 34.8% (after 25 h), M_n = 8100, and M_w/M_n = 1.09 (GPC).

A similar procedure was followed when other conditions were applied in the homopolymerization.

Preparation of Monofunctional Macroinitiator (PBA-Br). A 17.94 g (140 mmol) amount of *n*-butyl acrylate and 3.0 mL of anisole (GC standard for conversion measurement) were placed into a 25 mL Schlenk flask covered with rubber septa, and the mixture was purged with nitrogen for 20 min. A 29.2 μL (0.14 mmol) amount of PMDETA and 31.2 μL (0.28 mmol) of MBrP were then added through a microsyringe, and the mixture was degassed again with nitrogen for 10 min to remove air. Finally, 20.1 mg (0.14 mmol) of CuBr was placed into the solution, and it was degassed by three freeze−pump−thaw cycles. The resulting mixture was immersed in a silicone oil bath preheated to 70 °C. After 23 h the polymer solution was diluted with 100 mL of THF. The diluted THF solution was passed through an alumina column to remove the catalyst. The pure viscous tacky polymer was obtained after removing the THF solvent under reduced pressure at 30 °C over 24 h using a vacuum pump. GC analysis for the polymer solution diluted with THF showed that the monomer conversion was 57%. M_n = 42 100 and M_w/M_n = 1.14 (GPC).

Preparation of Difunctional Macroinitiator (Br-PBA-Br). A difunctional macroinitiator was prepared under the same conditions used in the synthesis of the above-mentioned monofunctional macroinitiator, except that 17.18 mL (120 mmol) of BA and 71.1 μL (0.3 mmol) of DMDBHD were used instead of MBrP as an initiator; 43 mg (0.03 mmol) of CuBr, 62.6 μL (0.3 mmol) of PMDETA, and 10 h of polymerization time were used. The monomer conversion was 50% (GC). M_n = 24 700 and M_w/M_n = 1.13 (GPC).

Synthesis of AB-Type Diblock Copolymers (PBA-*b*-PCAEMA). A 0.518 g (0.0123 mmol) amount of PBA-Br (M_n = 42 100), 281 mg (0.741 mmol, 0.15 mol/L in terms of the solvent) of CAEMA, and 5.0 mL of anisole solvent were placed into a 10 mL Schlenk flask covered with rubber septa and stirred for 1 h at room temperature while purging with nitrogen. A 6.7 μL (0.0246 mmol) amount of HMTETA was added to the resulting solution through a microsyringe, and then the mixture was degassed with nitrogen for 10 min. Finally, 2.43 mg (0.0246 mmol) of CuCl was placed into the reaction mixture, which was then degassed by three freeze−pump−thaw cycles. An initial sample (0.1 mL) was removed as GPC standard for conversion measurement before copolymerization. The orange-colored solution was immersed into a silicone oil bath preheated to 80 °C for polymerization under nitrogen atmosphere. After a given time, a sample of the polymer solution in anisole was removed by a syringe for GPC analysis. The purification procedure was the same as that used above for the homopolymer to get a yellowish, AB-type, PBA-*b*-PCAEMA block copolymer. The conversion of the CAEMA for the LC block was 35.3% after a polymerization time of 91 h. M_n = 50 500 and M_w/M_n = 1.16 (GPC).

Other diblock copolymers with different compositions were prepared using similar procedures.

Synthesis of ABA-Type Triblock Copolymers (PCAEMA-*b*-PBA-*b*-PCAEMA). The triblock copolymers were prepared using the same method as in the synthesis of the diblock copolymers, except that 0.466 g (1.230 mmol, 0.3 mol/L in terms of the solvent) of CAEMA, and 0.507 g (0.0205 mmol) of the difunctional macroinitiator Br-PBA-Br (M_n = 24 700) instead of the monofunctional macroinitiator were employed along with 4.1 mg (0.041 mmol) of CuCl, 1.1 μL (0.041 mmol) of PMDETA, and 4.1 mL of anisole. The conversion of the CAEMA for the LC blocks was 86.7% when the polymerization time was 120 h. M_n = 41 500 and M_w/M_n = 1.24 (GPC).

Other triblock copolymers with different compositions were synthesized by changing the molar ratio of the LC monomer to the difunctional macroinitiator.

Preparation of Thin Films of Block Copolymers. Thin film samples of block copolymers were prepared by either spin coating the polymer solution (1.0 mg/1.0 mL) in THF (or chloroform) at 2000 rpm for 5 min or solvent casting. Surface morphology of thin films was studied at room temperature by atomic force microscopy.

Results and Discussion

Preparation of LC Homopolymer and Block Copolymers. ATRP was successfully used to prepare LC homopolymers from the LC monomer with azobenzene moiety (CAEMA) and to synthesize the range of new LC block copolymers with the LC block as a hard segment and soft PBA block (Table 1). To investigate

Scheme 2. Synthetic Route for Diblock Copolymer

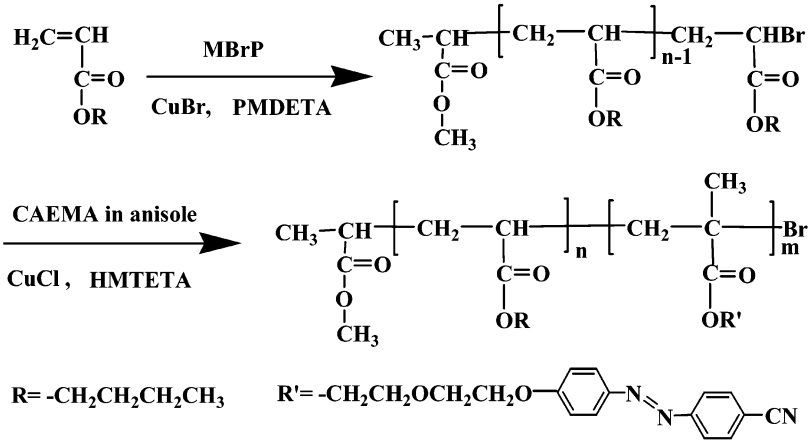

Scheme 3. Synthetic Route for Triblock Copolymer

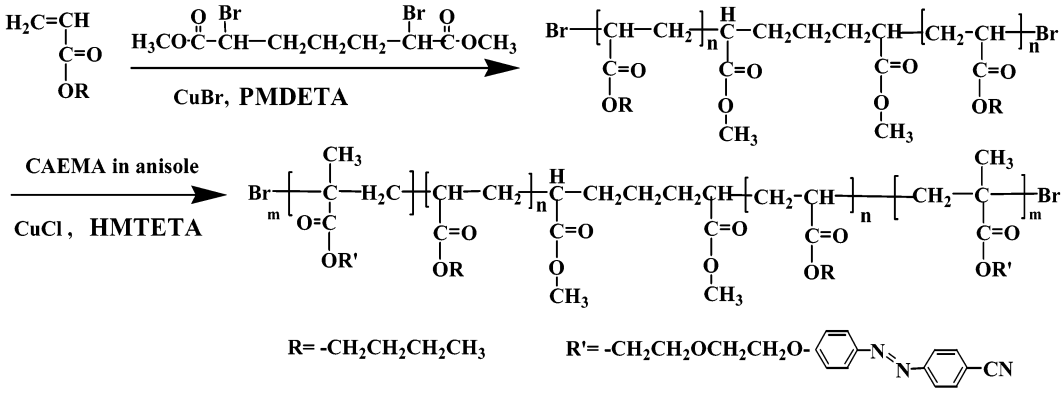

the influence of molecular weight on phase-transition temperatures,[27] three LC homopolymers with different degrees of polymerization were first synthesized by changing polymerization conditions. As shown in Scheme 1, the homopolymer was prepared by using EBriB, CuCl or CuBr, and HMTETA as initiator, catalyst, and ligand, respectively. The use of CuCl as a catalyst at 80 °C gave a homopolymer with a controlled number-average molecular weight, M_n= 8100 g/mol, and a low polydispersity, M_w/M_n=1.09. Increasing the polymerization temperature to 90 °C increased the molecular weight to 11 900, still preserving the polydispersity at 1.10. The number-average molecular weights were very close to the theoretically calculated values, indicating that the homopolymerization was well controlled using the CuCl/HMTETA catalyst. On the other hand, the use of CuBr under the same conditions, resulted in preparation of a homopolymer with a lower molecular weight, M_n= 5500. Better control with CuCl could be due to more efficient initiation via halogen exchange.[43]

Subsequently, the mono- and difunctional PBA macroinitiators were prepared using ATRP to make di- and triblock copolymers composed of the LC and PBA segments, as shown in Schemes 2 and 3. Monofunctional PBA macroinitiator with one bromine group at the end of the polymer chain was synthesized using MBrP, CuBr, and PMDETA at 70 °C. Difunctional PBA macroinitiator with bromine groups at both ends of the polymer chain was prepared by using DMDBHD as an initiator instead of MBrP under similar conditions. The number-average molecular weights of PBA-Br and Br-PBA-Br were 42 100 and 24 700, respectively.

The prepared mono- and difunctional macroinitiators with low polydispersity (1.13 and 1.14) were used to form the corresponding di- and triblock copolymers. Two diblock and three triblock copolymers were prepared by controlling the molar feed ratio of the LC monomer to the mono- or difunctional macroinitiators. The number-average molecular weights of the resulting copolymers increased with time and the concentration of second monomer. The polydispersities increased as the molecular weights increased. Such a trend could be due to slower diffusion in viscous media or chain-breaking reactions.

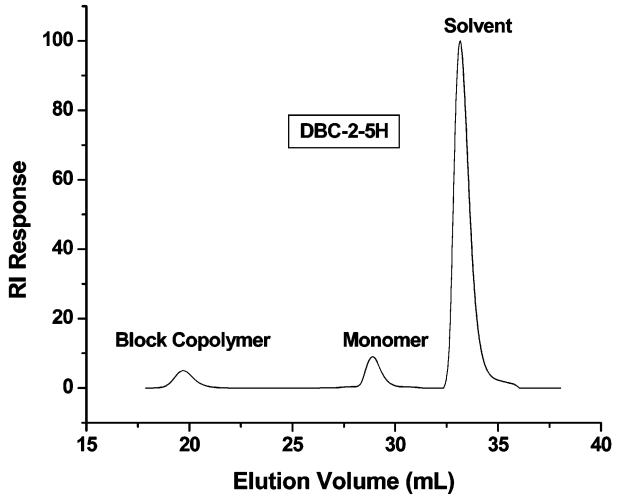

Figure 1. Representative GPC curve of the diblock copolymer (DBC-2) with elution time.

Figure 1 shows a representative GPC trace vs elution time for one of the block copolymers, DBC-2. Conversion of the LC monomer during the block copolymerization

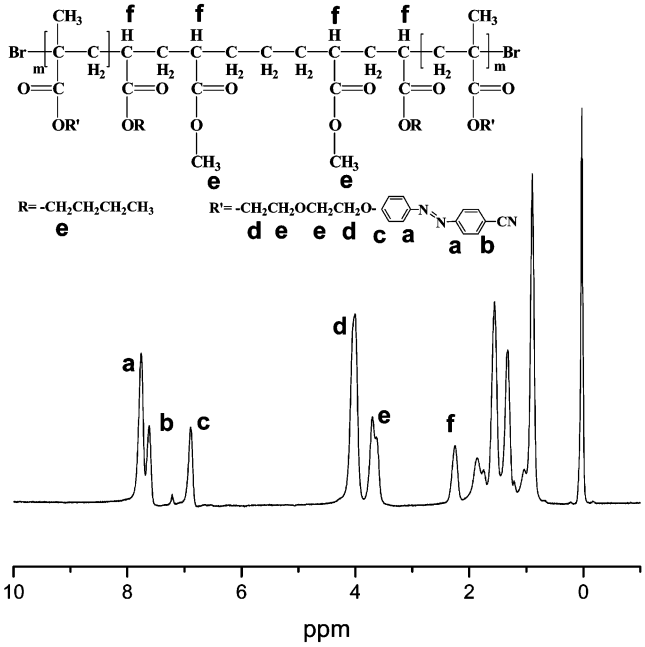

Figure 2. ^{1}H NMR spectrum of the triblock copolymer (TBC-3) in $CDCl_3$ solvent.

was estimated from examination of the ratio of the areas of the peaks corresponding to the monomer and the solvent anisole (standard) appearing at 28 and 33 min. For all the polymers the number-average molecular weights obtained from GPC measurements using PS standards were very close to the values predicted from analysis of the conversion data. This indicates that the block copolymerization by ATRP proceeds in a well-controlled manner. Figure 2 displays the ^{1}H NMR spectrum for one of the block copolymers, TBC-3; the composition of the LC block in the di- and triblock copolymers was calculated from the ratio of the indicated characteristic peaks. The LC contents were in the range of 15−55% as summarized in Table 1.

The dependence of the degree of polymerization on time or conversion was examined by following the evolution of molecular weight of di- and triblock copolymers with conversion (Figures 3−5). For all the block copolymers, the GPC traces shifted to high molecular weights with the increase of polymerization time (Figures 3a, 4a, and 5a), implying the well-controlled, living character of the reaction. Every curve had a narrow unimodal shape, suggesting that the mono- and difunctional macroinitiators used as chain extenders acted efficiently to initiate the block copolymerization.[28,44] In the diblock copolymerization conversion of the LC block increased linearly over the 44 h reaction time frame. The molecular weight varied linearly with time and conversion, indicating the controlled/living character of the diblock copolymerization (Figure 3a and 3b). The polydispersities of the AB type diblock copolymers (PBA-*b*-PCAEMA) were as low as 1.14−1.17 (Figure 3c).

Figures 4 and 5 show the results for the triblock copolymerization. Both number-average molecular weight and conversion for the LC block in the ABA type triblock copolymers (PCAEMA-*b*-PBA-*b*-PCAEMA) increased linearly with time for 48 h and then leveled off as in the diblock copolymerization (Figures 4b and 5b). The polydispersities of resulting copolymers were in the range from 1.13 to 1.24. The dependence of molecular weight on conversion was linear, as shown in Figures

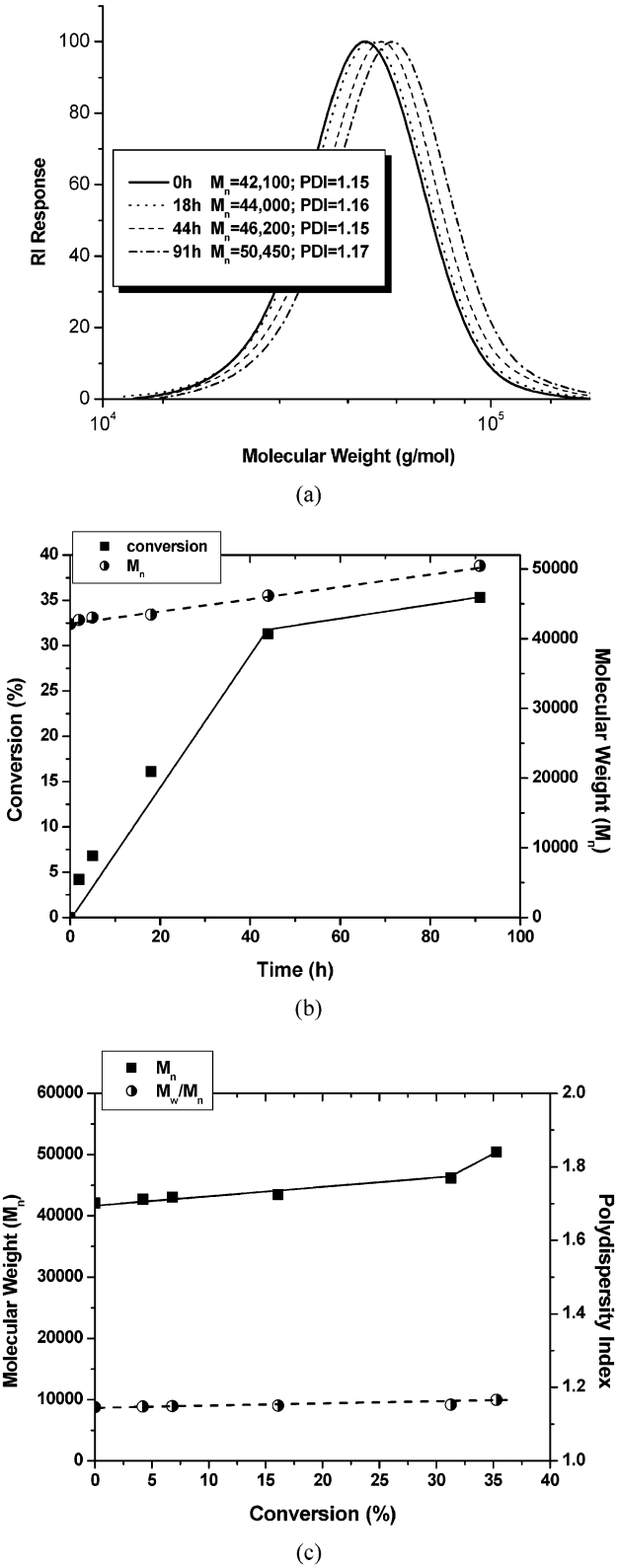

Figure 3. Molecular weight evolution during preparation of the diblock copolymer: (a) GPC traces for the BP-1, (b) dependence of conversion and molecular weight on time, (c) dependence of molecular weight and polydispersity on conversion.

4c and 5c. This indicates that the difunctional macroinitiator was efficient as a chain extender for preparation of the ABA-type triblock copolymer having LC A blocks. On the basis of these results, three kinds of triblock copolymers with LC block contents 17.5%,

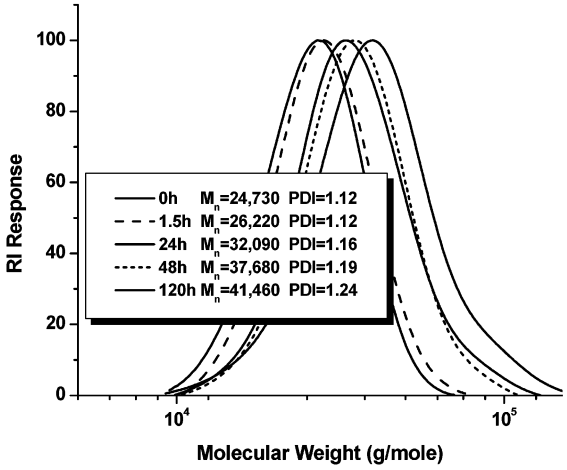

(a)

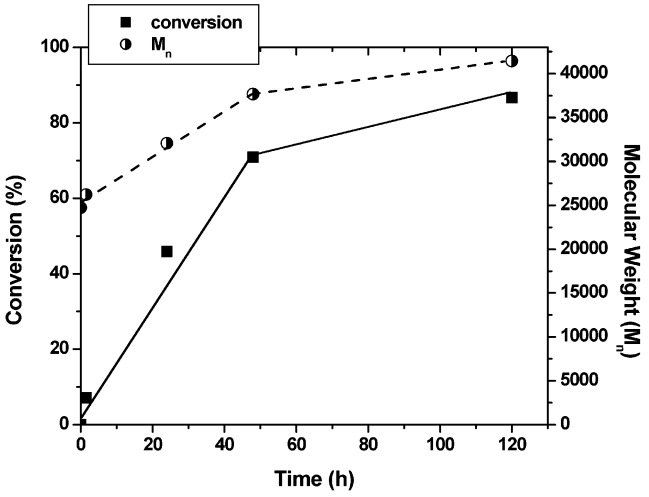

(b)

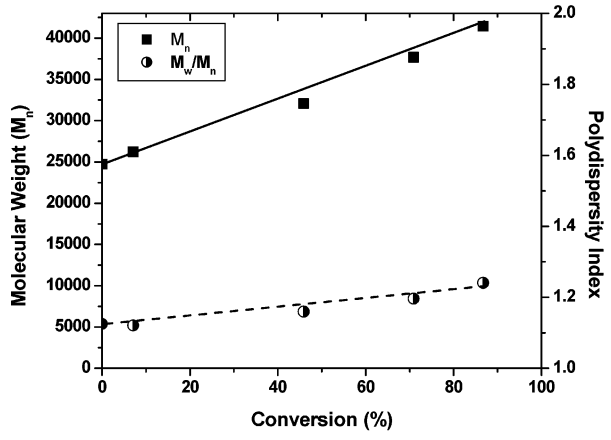

(c)

Figure 4. Molecular weight evolution during preparation of the triblock copolymer: (a) GPC traces for the TBC-2, (b) dependence of conversion and molecular weight on time, (c) dependence of molecular weight and polydispersity on conversion.

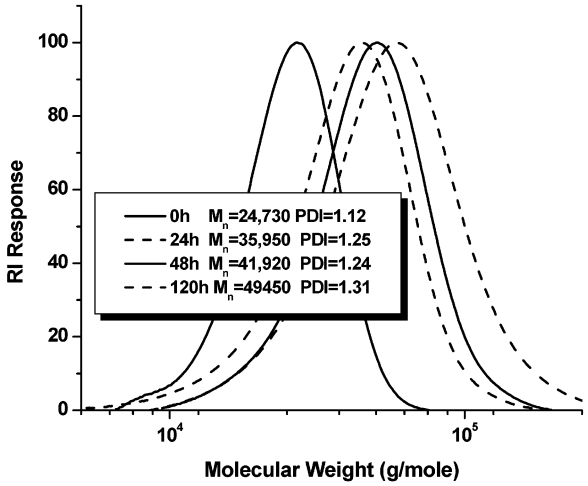

(a)

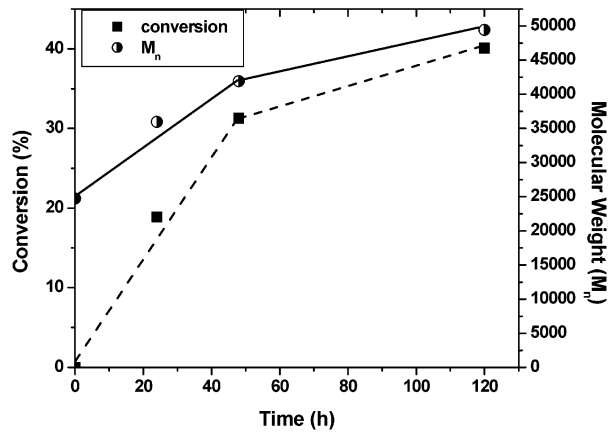

(b)

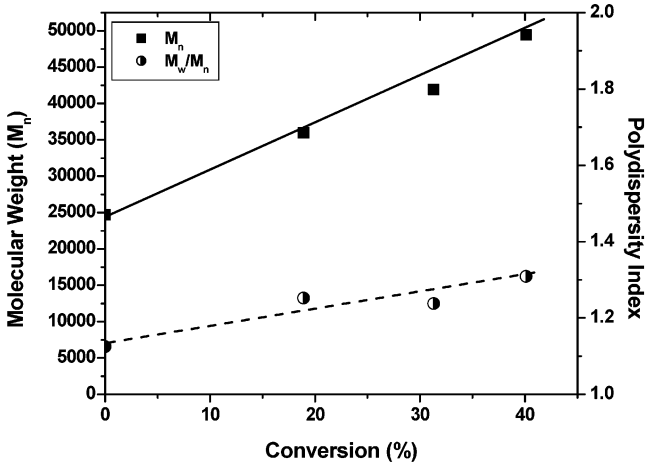

(c)

Figure 5. Molecular weight evolution during preparation of the triblock copolymer: (a) GPC traces for the TBC-3, (b) dependence of conversion and molecular weight on time, (c) dependence of molecular weight and polydispersity on conversion.

38.7%, and 53.4% were prepared by changing the molar feed ratio of the LC monomer to the difunctional macroinitiator from 30/1 to 60/1 to 160/1, respectively.

Thermal Phase Transitions and LC Textures. Phase-transition temperatures and liquid-crystalline textures of the monomer and all the polymers were investigated by means of optical polarizing microscopy (OPM) and DSC. Figure 6 shows the liquid-crystalline textures of the monomer CAEMA at different temperatures during the cooling cycle. Of particular interest here is the appearance of micrometer-sized thread-like fibrils at 110 °C (most likely of nematic character) and the significant increase in their number between 110 and 52 °C. Subsequently, annealing the monomer at 45 °C for 2 h changed the fibrils to a homogeneous smectic

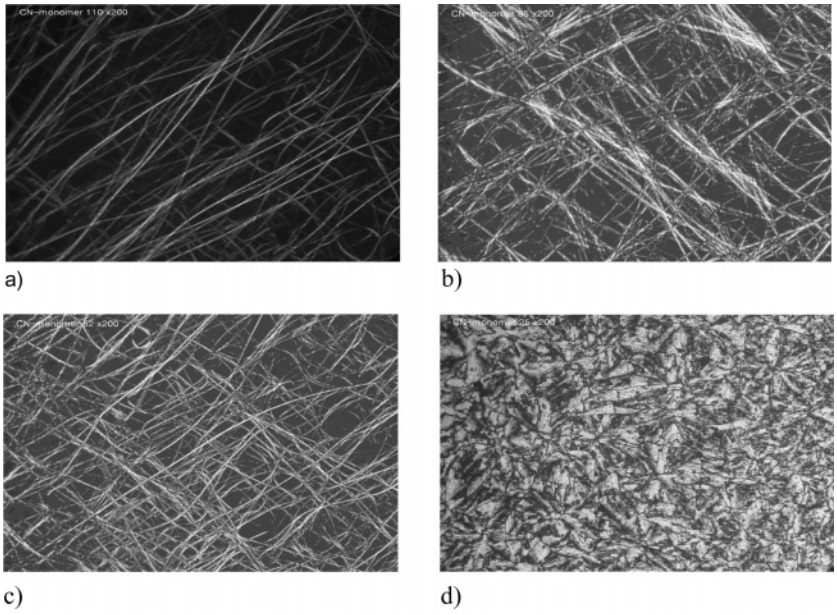

Figure 6. Liquid-crystalline textures of the monomer CAEMA at different temperatures: (a) 110 °C, (b) 85 °C, (c) 52 °C, (d) annealed at 45 °C for 2 h. Magnification = ×200.

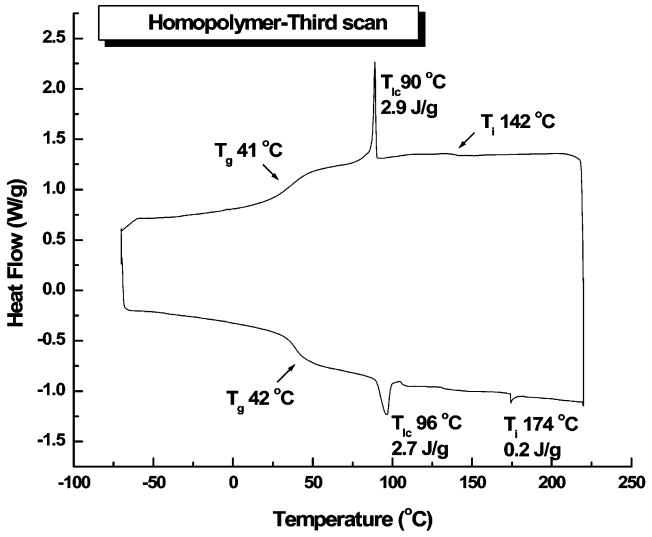

Figure 7. DSC thermogram of the homopolymer (HP-1).

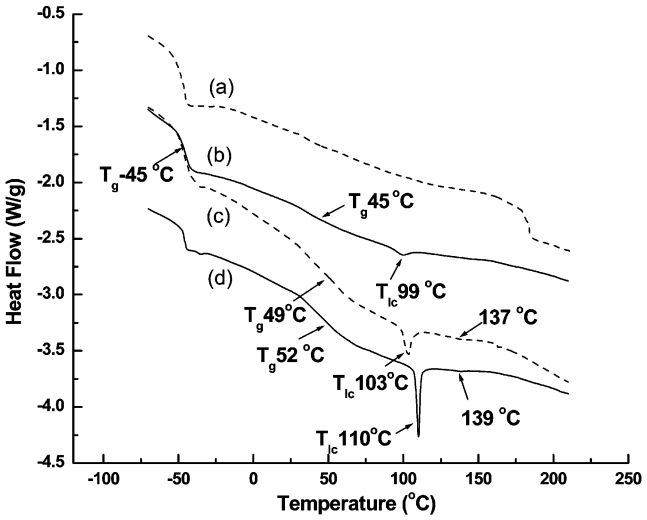

Figure 8. DSC thermograms of the block copolymers with different contents of the LC block: (a) DBC-2-15.8%, (b) TBC-1-17.5%, (c) TBC-2-38.7%, (d) TBC-3-53.4%.

phase with a typical fan-shaped focal conic texture. This indicates not only that the temperature range for the formation of liquid-crystalline phase is very broad, but also that the rate of its formation is very slow, quite unusual for typical liquid-crystalline compounds.

Accordingly, DSC thermograms of the monomer obtained upon cooling revealed a very weak broad exothermic transition at 115 °C and a sharp crystallization peak at 42 °C. The weak exothermic peak most likely corresponds to the transition from isotropic to nematic phase (T_{I-N}), whereas the sharp one is due to the transition from smectic phase to crystalline state, as observed by OPM. On heating, only two weak, broad transitions at 52 and 73 °C were observed. Such behavior indicates that the monomer exhibits enantiotropic liquid crystallinity, i.e., the instance when the liquid-crystalline phase is present both on heating and cooling.

Typical third DSC traces of the homopolymer HP-1 are shown in Figure 7. Strong and weak mesophase transitions during both heating and cooling cycles were observed. The strong and sharp transition in the lower temperature range was assigned to a smectic−nematic transition (T_{S-N}); the weak feature observed at higher temperatures was identified as a nematic to isotropic transition (T_{N-I}). In addition, the glass transition of the homopolymer was observed around 40 °C. These results are somewhat different from those described in the literature,[41] pointing to the modification of liquid-crystalline block phase transition conditions in the copolymer system.

Figure 8 shows the second DSC heating traces for the di- and triblock copolymers. The two triblock copolymers TBC-2 and -3 (Figure 8c and d) had relatively large endothermic transitions (T_{S-N}) at 103 and 110 °C, and they also showed very small mesophase transitions (T_{N-I}) between 135 and 140 °C. The presence of these transitions was confirmed by additional experiments performed using a more sensitive modulated DSC

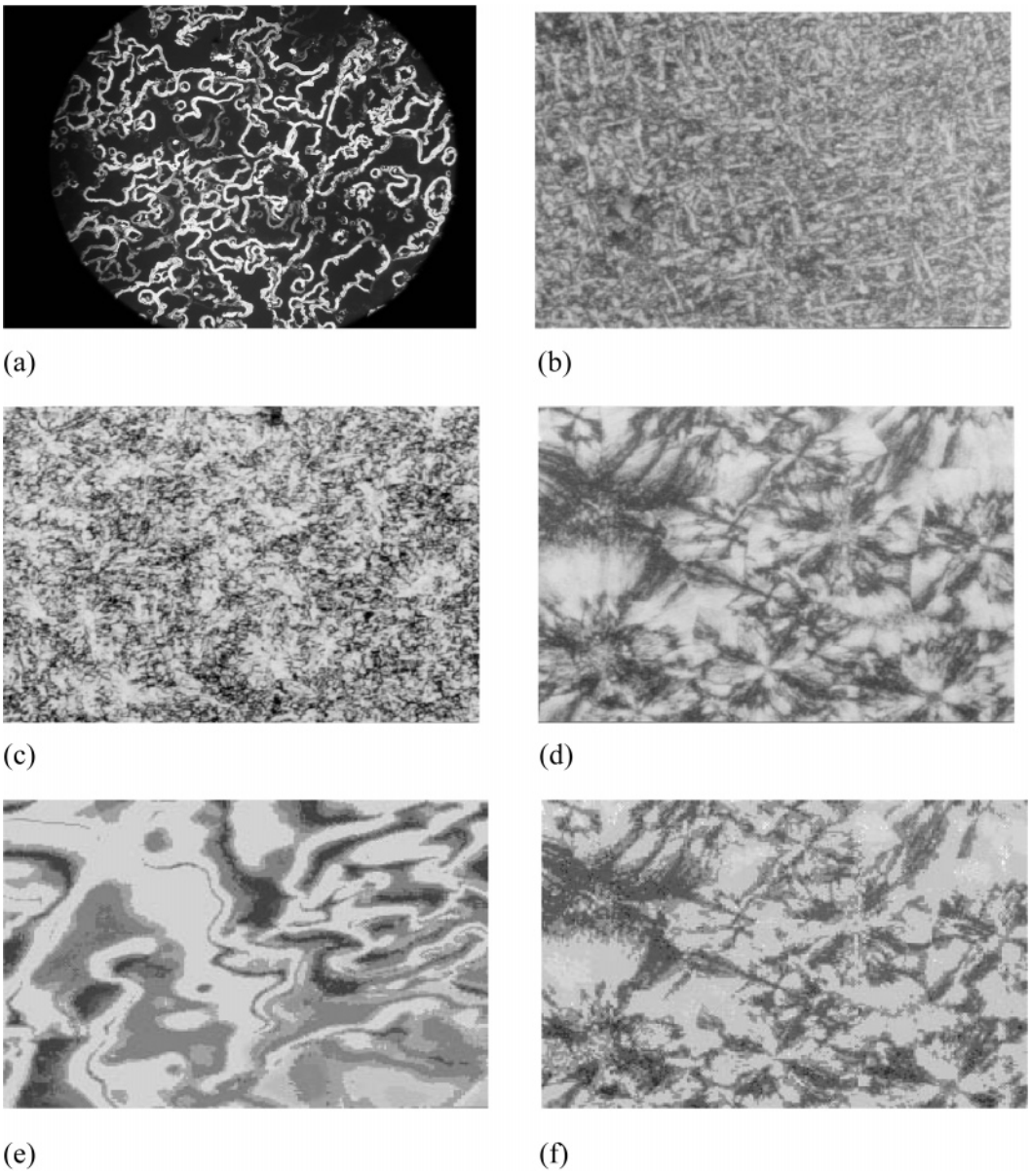

Figure 9. Liquid-crystalline textures of the homopolymer and the triblock copolymers: (a) HP-1-48 °C, (b) HP-1-annealed-47 °C-2 h, (c) TBC-2-annealed-116 °C-6 h, (d) TBC-2-95 °C, (e) TBC-3-annealed-122 °C-4 h, (f) TBC-3-70 °C. Magnification = ×200 except for a where ×100.

Table 2. Thermal Transition Data for the LC Homopolymer and the Block Copolymers Prepared by ATRP

	phase transition temperature (°C) and corresponding enthalpy changes (J/g)[a]									
	second heating					first cooling				
CAEMA		K52	73(7.6)		I	I115(-0.3)	N *	S42(−8.8)	k	
HP-1		g42	S 96(2.8)	N174(0.2)	I	I142	N 90(−2.9)	S41	g	
DBC-1	g-46	g*	S*	N184(0.42)	I	I133(-0.2)	N*	S43	g-**56**	g
TBC-1	g-45	g45	S 99(0.26)	N*	I	I*	N 94(-0.33)	S48	g-**56**	g
TBC-2	g-45	g49	S103(0.44)	N137	I	I144	N102(-0.5 9)	S49	g-**58**	g
TBC-3	g-45	g52	S110(1.73)	N139(0.15)	I	I145	N107(-1.9)	S58	g-**59**	g

[a] K= crystalline phase; S = smectic phase; N = nematic phase; g = glassy phase; I = isotropic. Asteisk (*) indicates not detected.

instrument (TA DSC-Q100, data not shown). In contrast, for the triblock copolymer TBC-1 (Figure 8b) with the lowest composition of the LC block, only one weak feature, assigned to the smectic−nematic transition was observed at T_{S-N} = 99 °C. In addition to the upward shift of T_{S-N}, triblock systems exhibited also an increase of the glass-transition temperature. The endothermic transition for these systems also shifted upward and increased its strength with an increase of the LC block content from 17.5% to 53.4%, as expected for the increase of the molecular weight of the LC segments.[27,45] In addition, the di- and triblock copolymers showed around −45 °C the glass-transition temperature of the PBA segments used as macroinitiators. These transition temperatures and the corresponding enthalpy changes for all samples are summarized in Table 2, and they also show trends similar to those described in the literature.[27, 44]

The structure of the LC phases for all the copolymers was studied on the first cooling cycle using OPM, as

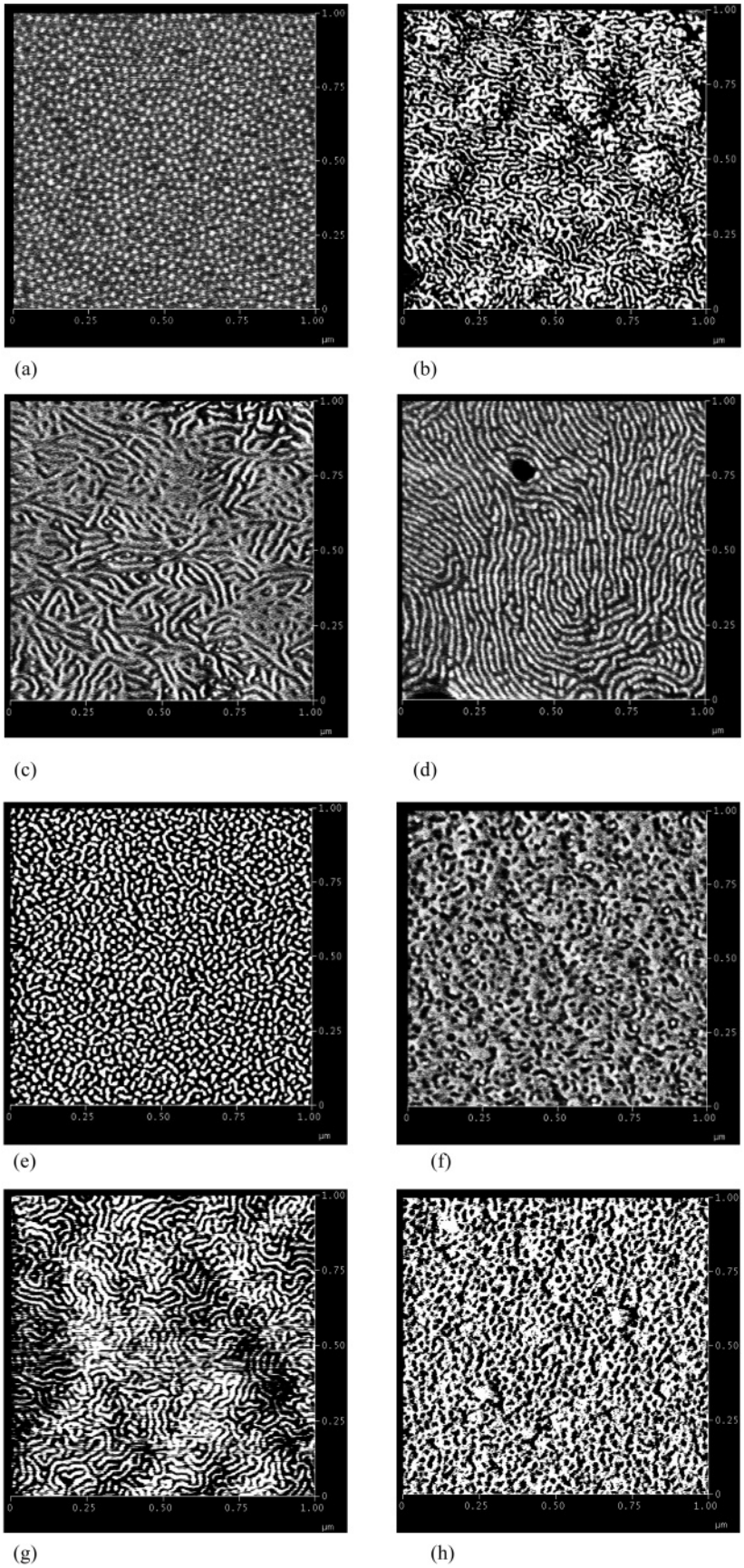

Figure 10. Tapping-mode AFM images of block copolymer films with different LC block contents: (a) DBC-2-THF-SC, (b) TBC-1-THF-SC, (c) TBC-1-THF-SC-100 °C, (d) TBC-1-$CHCl_3$-SC, (e) TBC-1-$CHCl_3$-SpC, (f) TBC-2-THF-SC, (g) TBC-2-THF-SC-100 °C, (h) TBC-3-$CHCl_3$-SpC-110 °C. All images represent cantilever phase shift maps with the vertical scale range of 10°.

shown in Figure 9. The thread-like fibrils which appeared in the homopolymer at 48 °C (Figure 9a) changed upon annealing at 47 °C for 2 h into the smectic structure with a typical rodlike texture (Figure 9b).

Such behavior resembles one observed for the monomer. On the other hand, annealing the TBC-2 for 6 h and TBC-3 for 4 h showed a typical Schlieren texture with two or four brushes, a nematic structure, in the range of mesophase transition temperature (T_{I-N}) on cooling cycle (Figure 9c, e).[46] Subsequently, cooling to the lower temperature range of 95−70 °C changed their nematic structures to smectic ones such as fan-shaped focal conic textures (Figure 9d, f). In contrast, OPM studies of DBC-2 and TBC-1 did not reveal any textures, most likely due to the low concentrations of the LC segments in these copolymers.

Nanoscale Morphology of Block Copolymers. In general, block copolymers with incompatible segments produce characteristic microphase-segregated nanostructures such as spheres, cylinders, gyroids, and lamellae. The type of nanostructure typically depends on the volume fractions of different segments and on the extent of their incompatibility.[47] With the systems containing crystallizable and/or mesogenic segments, such as the copolymers being the subject of this study, the interplay between segment ordering and nanoscale morphology is of particular interest.[48] Morphology of thin films of block copolymers with LC hard segments prepared in this study and its dependence on physical factors such as solvent, different casting procedures (solvent casting or spin coating), temperature, and composition ratio were studied with the aid of tapping-mode atomic force microscopy (TMAFM). TMAFM is particularly useful in the studies of block copolymers containing soft and hard segments, since without any additional sample treatment it can easily contrast surface regions characterized by different mechanical properties. AFM observations are restricted to (sub)-surface regions of materials, and they have to be used with caution when information about bulk nanostructure is desired. Moreover, surface (and bulk) morphologies of block copolymers frequently exhibit dependence on thermal/processing history, often due to kinetic trapping of metastable structures. As will be described below, these effects were manifested prominently in materials being the subject of this study.

All samples that were the subject of this study produced particularly good contrast in so-called phase images, which map the phase shift between the cantilever deflection and the signal used to drive its oscillation. This is not surprising since the phase shift is particularly sensitive to the differences in energy dissipation in tip sample interactions (mechanically lousy soft PBA vs elastic, rigid LC blocks).[49] In all presented images the dark end of phase gray scale corresponds to larger phase shifts, indicating regions of higher energy dissipation. TMAMF images of thin films of different diblock and triblock copolymers with different fractions of LC segments prepared by solvent casting (SC) or spin coating (SpC) using different solvents are shown in Figure 10. Regardless of preparation conditions, the images of diblock copolymer DBC-2 containing 15.8% of the LC block revealed the presence of hexagonally arranged bright round domains (center-to-center spacing $\approx$ 22 nm) surrounded by continuous dark regions (Figure 10a). Such morphology is consistent with spheres or end-on cylinders of LC blocks embedded in the PBA matrix. In contrast, the morphology of triblock copolymers varied significantly, depending on the film preparation conditions and the fraction of LC segment in the block copolymer (Figure 10 b−h). For example, upon casting from THF, triblock TBC-1, with a similar overall composition as diblock DBC-2, formed extensively branched surface morphology (Figure 10b). After annealing at 100 °C, in the vicinity of the T_{S-N} temperature, this morphology gave way to distinctly shaped more elongated domains, suggesting the shift toward lamellar structure. Similar transition with annealing was observed for triblock TBC-2 with higher concentration of the LC block (38.7%) cast from THF (Figure 10f and g). Interestingly, when TBC-1 was cast from chloroform rather than THF, it right away formed more stable lamellar morphology (Figure 10d), presumably due to less extensive kinetic trapping at the lower evaporation rate of chloroform. This kinetic argument was supported by the results of observations of the same sample prepared by spin coating. Under rapid solidification conditions accompanying this process, the lamellar morphology was replaced by what appeared to be the mixture of spheres and short cylinders (Figure 10e). These results indicate that copolymers under study can be easily trapped in metastable morphologies, most likely stabilized by the liquid-crystalline order of hard segments. Equilibration of morphology with annealing in the vicinity of smectic−nematic transition is consistent with the removal of trapping constraints imposed by the smectic order. In this context it is particularly interesting to notice that despite numerous attempts, the triblock TBC-3 with the highest LC block content (53.4%) always produced the similar extensively branched morphology (Figure 10h). Such behavior may indicate the overwhelming influence of liquid-crystalline hard blocks on the phase structure of the copolymer.

Conclusions

Well-controlled homopolymers and block copolymers were prepared from a monomer with LC *p*-cyanoazobenzene moieties as a substituent. The homopolymers and block copolymers, with the LC monomer as the hard segment and PBA as the soft one, were prepared by ATRP. The (co)polymers displayed low polydispersity, $M_w/M_n < 1.3$, and had a typical smectic structure with fan-shaped focal conic textures. The molecular weights of the LC (co)polymers increased linearly with conversion, confirming the controlled/living characteristic of ATRP. PBA mono- and difunctional macroinitiators were prepared and efficiently initiated the block copolymerization with the LC monomer units. The nanoscale morphology of thin films of block copolymers cast from different solvents using different casting procedures was examined by atomic force microscopy. The morphology of the block copolymer films depended on the preparation method and film-forming conditions as well as the composition ratio of the LC and PBA segments. The particularly strong dependence of nanoscale structure on sample preparation conditions and thermal history was attributed to the stabilization of metastable structures by liquid-crystalline order of hard blocks.

Acknowledgment. K.M. acknowledges support of the National Science Foundation (DMR00-90409). Y.K.H. thanks the Korea Research Foundation for financial support within the BK 21 Program for the Center for Functionalized Organics and Organic-Inorganics, Department of Chemistry, Hanyang University.

References and Notes

(1) In *Advances in Controlled/Living Radical Polymerization*; Matyjaszewski, K., Ed.; American Chemical Society: Washington, D.C., 2003; Vol. 854.

(2) Matyjaszewski, K.; Davis, T. P. *Handbook of Radical Polymerization*; Wiley- Interscience: Hoboken, 2002.
(3) Wang, J. S.; Matyjaszewski, K. *J. Am. Chem. Soc.* **1995**, *117*, 5614.
(4) Matyjaszewski, K.; Xia, J. *Chem. Rev.* **2001**, *101*, 2921.
(5) Kamigaito, M.; Ando, T.; Sawamoto, M. *Chem. Rev.* **2001**, *101*, 3689.
(6) Qiu, J.; Matyjaszewski, K. *Macromolecules* **1997**, *30*, 5643.
(7) Wang, J.-L.; Grimaud, T.; Matyjaszewski, K. *Macromolecules* **1997**, *30*, 6507.
(8) Davis, K.; Paik, H.-j.; Matyjaszewski, K. *Macromolecules* **1999**, *32*, 1767.
(9) Matyjaszewski, K.; Jo, S. M.; Paik, H.-j.; Gaynor, S. G. *Macromolecules* **1997**, *30*, 6398.
(10) Teodorescu, M.; Matyjaszewski, K. *Macromol. Rapid Commun.* **2000**, *21*, 190, 194.
(11) Neugebauer, D.; Matyjaszewski, K. *Macromolecules* **2003**, *36*, 2598.
(12) Coessens, V.; Pintauer, T.; Matyjaszewski, K. *Prog. Polym. Sci.* **2001**, *26*, 337.
(13) Qiu, J.; Charleux, B.; Matyjaszewski, K. *Prog. Polym. Sci.* **2001**, *26*, 2083.
(14) Patten, T. E.; Xia, J.; Abernathy, T.; Matyjaszewski, K. *Science* **1996**, *272*, 866.
(15) Matyjaszewski, K.; Patten, T. E.; Xia, J. *J. Am. Chem. Soc.* **1997**, *119*, 674.
(16) Patten, T. E.; Matyjaszewski, K. *Adv. Mater.* **1998**, *10*, 901.
(17) Matyjaszewski, K.; Ziegler, M. J.; Arehart, S. V.; Greszta, D.; Pakula, T. *J. Phys. Org. Chem.* **2000**, *13*, 775.
(18) Davis, K. A.; Matyjaszewski, K. *Adv. Polym. Sci.* **2002**, *159*, 2.
(19) Matyjaszewski, K.; Teodorescu, M.; Acar, M. H.; Beers, K. L.; Coca, S.; Gaynor, S. G.; Miller, P. J.; Paik, H.-J. *Macromol. Symp.* **2000**, *157*, 183.
(20) Matyjaszewski, K.; Beers, K. L.; Woodworth, B.; Metzner, Z. *J. Chem. Educ.* **2001**, *78*, 547.
(21) Shipp, D. A.; Wang, J.-L.; Matyjaszewski, K. *Macromolecules* **1998**, *31*, 8005.
(22) Matyjaszewski, K.; Shipp, D. A.; McMurtry, G. P.; Gaynor, S. G.; Pakula, T. *J. Polym. Sci., Part A: Polym. Chem.* **2000**, *38*, 2023.
(23) Tsarevsky, N. V.; Sarbu, T.; Gobelt B.; Matyjaszewski, K. *Macromolecules* **2002**, *35*, 6142.
(24) Tong, J. D.; Moineau, G.; Leclere, P.; Bredas, J. L.; Lazzaroni, R.; Jerome, R. *Macromolecules* **2000**, *33*, 470.
(25) Qin, S.; Saget, J.; Pyun, J.; Jia, S.; Kowalewski, T.; Matyjaszewski, K. *Macromolecules* **2003**, *36*, 8969.
(26) Walter, M.; Faulhammer, H.; Finkelmann, H. *Macromol. Chem. Phys.* **1998**, *19*, 223.
(27) He, X.; Zhang, H.; Yan, D.; Wang, X. *J. Polym. Sci., Part A: Polym. Chem.* **2003**, *41,* 2854.
(28) Tian, Y.; Watanabe, K.; Kong, X.; Abe, J.; Iyoda, T. *Macromolecules* **2002**, *35*, 3739.
(29) Barbosa, C. A.; Coelho, M. R. G.; Gomes, A. S. *Macromol. Symp.* **2001**, *168*, 91.
(30) Chang, C.; Pugh, C. *Macromolecules* **2001**, *34*, 2027.
(31) Kasko, A. M.; Grunwald, S. R.; Pugh, C. *Macromolecules* **2002**, *35*, 5466.
(32) Serhatli, I. E.; Kacar, T.; Oenen, A. *J. Polym. Sci., Part A: Polym. Chem.* **2003**, *41*, 1892.
(33) Schneider, A.; Zanna, J. J.; Yamada, M.; Finkelmann, H.; Thoman, R. *Macromolecules* **2000**, *33*, 649.
(34) Moriya, K.; Seki, T.; Nakagawa, M.; Mao, G.; Ober, C. K. *Macromol. Rapid Commun.* **2000**, *21*, 1309.
(35) Natanson, A.; Rochon, P. *Chem. Rev*. **2002**, *102*, 4139.
(36) Han, M.; Ichimura, K. *Macromolecules* **2001**, *34*, 90.
(37) Hagen, R.; Bieringer, T. *Adv. Mater.* **2001**, *13*, 1805.
(38) Matyjaszewski, K.; Patten, T. E.; Xia, J. *J. Am. Chem. Soc.* **1997**, *119*, 674.
(39) Xia, J.; Matyjaszewski, K. *Macromolecules* **1997**, *30*, 7697.
(40) Han, Y. K.; Kim, D. Y.; Kim, Y. H. *J. Polym. Sci., Part A: Polym. Chem.* **1992**, *30,* 117.
(41) Andrews, S. R.; Williams, G.; Lasker, L.; Stumpe, J. *Macromolecules* **1995**, *28*, 8463.
(42) Allcock, R.; Kim, C. *Macromolecules* **1989**, *22*, 2596.
(43) Matyjaszewski, K.; Shipp, D. A.; Wang, J.-L.; Grimaud, T.; Patten, T. E. *Macromolecules* **1998**, *31*, 6836.
(44) Cui, L.; Zhao, Y. *Macromolecules* **2003**, *36*, 8246.
(45) Hao, X.; Heuts, J. P. A.; Barner-Kowollik, C.; Davis, T. P.; Evans, E. *J. Polym. Sci., Part A: Polym. Chem.* **2003**, *41,* 2949.
(46) Blumstein, A. *Polymer Liquid Crystals*; Plenum Press: New York and London, 1985; p 21−64.
(47) Bates, F. S.; Fredrickson, G. H. *Phys. Today* **1999**, *52*, 32−38
(48) Anthamatten, M.; Zheng, W. Y.; Hammond, P. T. *Macromolecules* **1999**, *32*, 4838.
(49) Garcia, R.; Perez, R. *Surf. Sci. Rep.* **2002**, *47*, 197−301.

MA0492059